ADA040470

Longitude-Time Pattern for Quiet-Time Midlatitude Electron Precipitation

~~Space Sciences Laboratory~~
The Ivan A. Getting Laboratories
The Aerospace Corporation
El Segundo, Calif. 90245

10 May 1977

Interim Report

Prepared for

SPACE AND MISSILE SYSTEMS ORGANIZATION
AIR FORCE SYSTEMS COMMAND
Los Angeles Air Force Station
P.O. Box 92960, Worldway Postal Center
Los Angeles, Calif. 90009

DDC
JUN 13 1977
B

AD No.
DDC FILE COPY

This interim report was submitted by The Aerospace Corporation, El Segundo, CA 90245, under Contract No. F04701-76-C-0077 with the Space and Missile Systems Organization, Deputy for Advanced Space Programs, P. O. Box 92960, Worldway Postal Center, Los Angeles, CA 90009. It was reviewed and approved for The Aerospace Corporation by G. A. Paulikas, Director, Space Sciences Laboratory. Lieutenant Dara Batki, SAMSO/YAPT, was the project officer for Advanced Space Programs.

This report has been reviewed by the Information Office (OI) and is releasable to the National Technical Information Service (NTIS). At NTIS, it will be available to the general public, including foreign nations.

This technical report has been reviewed and is approved for publication.

Dara Batki
Dara Batki, Lt, USAF
Project Officer

Joseph Gassmann
Joseph Gassmann, Major, USAF

FOR THE COMMANDER

Floyd R. Stuart
Floyd R. Stuart, Colonel, USAF
Deputy for Advanced Space Programs

REPORT DOCUMENTATION PAGE		READ INSTRUCTIONS BEFORE COMPLETING FORM
1. REPORT NUMBER SAMSO-TR-77-97	2. GOVT ACCESSION NO.	3. RECIPIENT'S CATALOG NUMBER
4. TITLE (and Subtitle) LONGITUDE-TIME PATTERN FOR QUIET-TIME MIDLATITUDE ELECTRON PRECIPITATION.		5. TYPE OF REPORT & PERIOD COVERED Interim rept.,
		6. PERFORMING ORG. REPORT NUMBER TR-0077(2260-20)-7
7. AUTHOR(s) Janet G. Luhmann and Alfred L. Vampola		8. CONTRACT OR GRANT NUMBER(s) F04701-76-C-0077
9. PERFORMING ORGANIZATION NAME AND ADDRESS The Aerospace Corporation El Segundo, Calif. 90245		10. PROGRAM ELEMENT, PROJECT, TASK AREA & WORK UNIT NUMBERS
11. CONTROLLING OFFICE NAME AND ADDRESS Space and Missile Systems Organization Air Force Systems Command Los Angeles, Calif. 90009		12. REPORT DATE 10 May 1977
		13. NUMBER OF PAGES 28
14. MONITORING AGENCY NAME & ADDRESS(if different from Controlling Office)		15. SECURITY CLASS. (of this report) Unclassified
		15a. DECLASSIFICATION/DOWNGRADING SCHEDULE

16. DISTRIBUTION STATEMENT (of this Report)

Approved for public release; distribution unlimited.

17. DISTRIBUTION STATEMENT (of the abstract entered in Block 20, if different from Report)

18. SUPPLEMENTARY NOTES

19. KEY WORDS (Continue on reverse side if necessary and identify by block number)

Electron Precipitation
Midlatitude Precipitation

$\leq$ or $=$

20. ABSTRACT (Continue on reverse side if necessary and identify by block number)

During geomagnetically quiet times, particle precipitation at midlatitudes $(2 \leq L \leq 4)$ results from a combination of pitch angle diffusion into the bounce loss cone and the opening of the bounce loss cone in the direction of drift to a maximum value which defines the drift loss cone. The geographical distribution of precipitation can thus be determined from geomagnetic field models which give the rate of change of the bounce loss cone size provided that an assumption is made about the spatial distribution of the source region where

DD FORM 1473
(FACSIMILE)

19. KEY WORDS *(Continued)*

20. ABSTRACT *(Continued)*

cont

particles are scattered into the drift loss cone. Some observations indicate that the pitch angle scattering of kilovolt electrons occurs preferentially in the 0600-1200 LT quadrant of the magnetosphere. If the source of drift loss cone electrons is localized, precipitation into the midlatitude atmosphere will depend on both longitude and time of day. A simple model, in which the morning source is represented by a delta function at 0800 LT, leads to a qualitative picture of the morphology of precipitation in both Northern and Southern Hemispheres. The predictions of this model are consistent with some observations of 29 and 59 keV electrons from the low altitude satellite 1972-76B.

PREFACE

The authors wish to thank H. C. Koons for initiating this research. The efficient computational assistance of L. M. Friesen is also gratefully acknowledged. Further benefit was derived from discussions with H. H. Hilton, J. B. Blake, G. A. Paulikas, I. J. Rothmuller and also B. T. Tsurutani, who provided unpublished data for our perusal.

CONTENTS

FIGURES

I. INTRODUCTION

The loss of radiation belt electrons from the plasmasphere is governed by the combined action of pitch angle scattering by turbulent electric and magnetic fields (see Lyons et al., 1972) and the well known windshield wiper effect (see Torr et al., 1975). Pitch angle scattering by ambient waves can inject stably trapped particles onto atmosphere-bound trajectories. The windshield wiper effect determines which trajectories are atmosphere-bound at a given geographic location.

A. Windshield Wiper Effect

The windshield wiper effect results from the asymmetry of the geomagnetic field. Because of this asymmetry, the bounce or atmospheric loss cone angle (Roederer, 1970), which marks the boundary between locally trapped and locally precipitating trajectories, is a function of longitude. This longitude dependence is particularly strong at L values inside of the plasmapause (L < 4).

Figure 1 shows how the size of the atmospheric loss cone at the equator varies with geographic longitude for several values of L. The ordinate gives the larger of the north or south 100 km loss cone angles as determined from a standard model of the geomagnetic field. Near the longitude of the South Atlantic Anomaly ($\sim 315^{\circ}$ - 360° E) the bounce loss cone at fixed L attains a maximum size which defines the drift loss cone angle. In general, particles which move at pitch angles smaller than this maximum value will precipitate into the atmosphere during their drift cycle. Those within the local bounce loss cone will precipitate locally. The remainder observed locally in the drift loss cone will probably be lost to the atmosphere as they drift toward the anomaly.
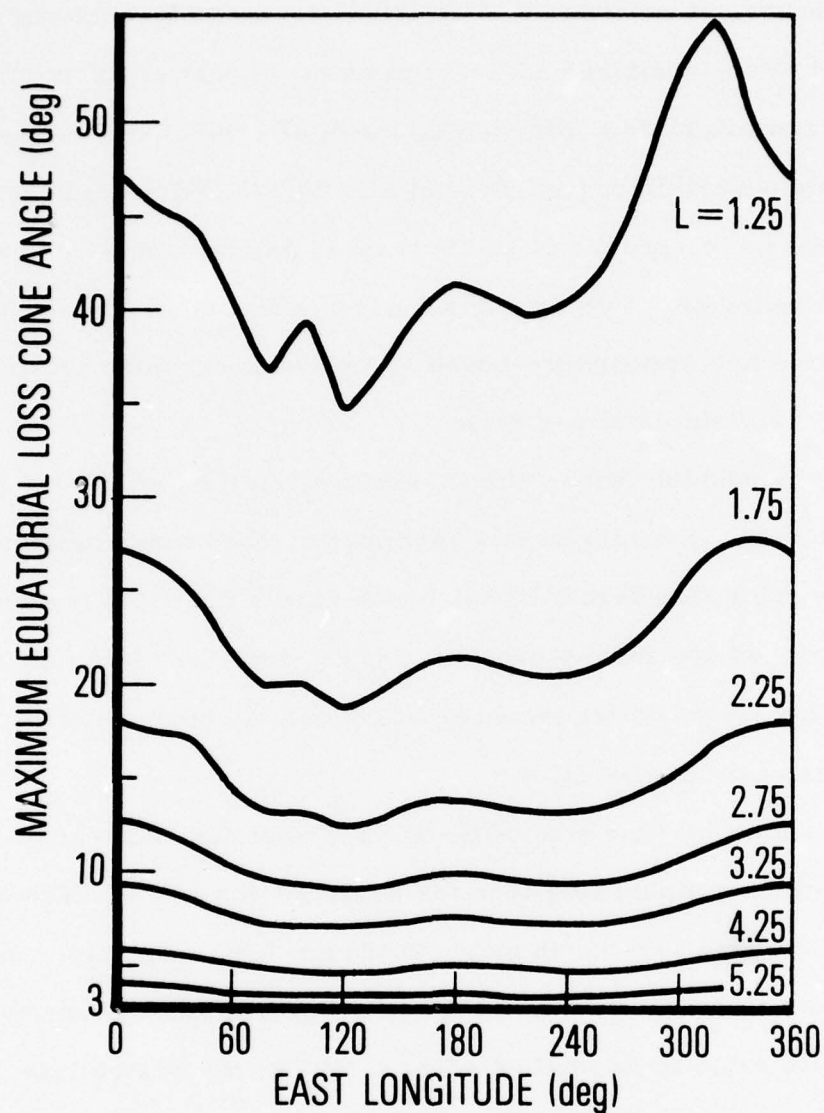
-7-

Figure 1. Larger of the North or South Equatorial Loss Cone Angles as Given by the IGRF 1965. 0 Geomagnetic Field Model (IAGA, 1969) Vs. Geographic Longitude Measured Eastward From the Prime Meridian.

-8-

Particles that are within the drift loss cone but outside of the local bounce loss cone are designated as quasitrapped. The quasitrapped and locally precipitating particles together comprise the drift loss cone population which acts as the reservoir for midlatitude precipitation (Paulikas, 1975). Precipitation that results from the increase of the bounce loss cone angle is attributed to the windshield wiper effect. In essence, the windshield wiper effect is a valve-like mechanism that controls the precipitation of the quasitrapped component of the drift loss cone population.

B. Pitch Angle Scattering

The source which replenishes the drift loss cone particles is not completely understood. Some early electron data (Williams and Kohl, 1965, Imhof, 1968) appeared to indicate that the quasitrapped population was replenished by an atmospheric source at all longitudes. Indeed, previous analyses have examined midlatitude precipitation from the point of view of an extended source model which assumes that pitch angle scattering into the drift loss cone occurs uniformly at all longitudes and times (Torr, et al., 1975).

An extended source viewpoint was also invoked in the theoretical treatment of stably trapped plasmasphere electrons (Lyons, et al., 1972) which included pitch angle scattering from wave-particle interactions (Kennel and Petschek, 1966). Lyons et al. (1972) and Lyons and Williams (1975) found that particle interactions with the electromagnetic waves that cause plasmaspheric hiss could produce the stably trapped electron pitch angle distributions that are observed at midlatitudes. While it is apparent that wave-particle interactions above 100 km can also play a role in filling the drift loss cone, the characteristics of the electromagnetic noise

-9-

that scatters the particles can have different implications for stably
trapped and quasitrapped populations. The assumption of uniform in-
jection is generally adequate in drift-averaged treatments which apply
to stably trapped electrons. However, quasitrapped electrons must be
generated less than a drift period before they are observed since they are
lost in the anomaly every drift cycle. As a result, the quasitrapped popu-
lation is sensitive to nonuniformities in the spatial distribution of the
scattering agency.

As pointed out by Imhof et al. (1976), many observations suggest
that quasitrapped electrons are generated primarily in a localized region
of the magnetosphere. Vampola et al. (1971) reported that the average
flux of > 300 keV outer zone electrons in the drift loss cone increases in
the morning after 0600 LT, reaching a maximum near 0900 LT. These
authors also observed a peak in the occurrence of ELF emissions near the
plasmapause in the time interval 0600-1200 LT. Mannan et al. (1975)
similarly observed intense outer zone ELF chorus in the time interval
0600-1000 LT. In two earlier experiments, Taylor and Gurnett (1968)
found an 0800-1000 LT maximum in VLF intensity and Dunckel and Helliwell
(1969) detected a morning enhancement in high altitude whistler noise.
Although many of these observations pertain to the high latitude extreme
of the L range that is under consideration here, they all suggest that a
localized region of strong pitch angle scattering is present in the morning
sector of the magnetosphere. This hypothesis is corroborated by the
recent observation by Imhof et al. (1976) that the energy spectra of >130 keV
slot region (L ≈ 2-3) electrons frequently develop peaks in the morning hours.

An explanation for the occurrence of enhanced wave-particle inter-
actions near the morning plasmapause was proposed by Brice and Lucas
(1971). These authors pointed out that dawn-dusk assymetries arise
naturally from the plasma convection pattern in the magnetosphere. The
outward flow of cold plasma from the ionosphere to the magnetosphere in
the morning hours can change the stable trapping limit for electrons. The
resulting unstable electrons produce whistler mode waves and undergo pitch
angle diffusion. Note that if these waves can propagate inside the plasma-
pause, the region in which scattering occurs can extend to arbitrarily low
L values.

Recently, Tsurutani et al. (1975) found evidences of enhanced scat-
tering of MeV electrons in the afternoon quadrant of the inner zone. In this
case, the data were obtained during periods of strong geomagnetic activity.
One can speculate that the position or spatial extent of the scattering region
in the magnetosphere is determined by the level of geomagnetic activity, the
morning location being characteristic of quiet conditions. Alternatively, the
source location may depend on electron energy, moving toward noon as the
energy increases. Although the present discussion is limited to the morning
source position, the application of the method of analysis to any source lo-
cation is trivial.

In this paper, the consequences of having both a temporally localized
source of drift loss cone electrons in the morning hours and a spatially
localized loss region in the vicinity of the anomaly are examined. It is
demonstrated that this combination produces a characteristic spatial and
temporal behavior of the electron population inside of the drift loss cone,
resulting in a unique pattern of precipitation into the midlatitude atmosphere.

-11-

In principle, the development that follows could also be applied to protons. However, the majority of quasitrapped inner zone protons are ring current protons which have been transported to low altitudes via charge exchange processes (Paulikas, 1975). Since the ring current source is distributed over all local times, low latitude proton precipitation can be described according to the model of Torr et al. (1975).

Particles in the drift loss cone are most easily observed at low altitudes. Figure 2 illustrates how a monoenergetic pitch angle distribution observed at 750 km is related to the distribution at the equator. A particle with an equatorial pitch angle outside of the drift loss cone mirrors above the observation point. As a result, all of the particles observed at several hundred kilometers and below are either quasitrapped or in the bounce loss cone. Observations of pitch angle distributions of electrons from the low altitude satellite 1972-76B, which had a nearly circular orbit at ~750 km, thus provided a data base for testing the morning source model. For the purpose of interpreting these data, the discussion includes an analysis of the low altitude pitch angle distributions that characterize a localized source.

EQUATOR (L≈2.75)

LOG $F_0(\alpha_0)$

EQUATORIAL PITCH ANGLE α_0

BOUNCE
DRIFT
LOSS CONE

750 km

BOUNCE ← DRIFT
LOSS CONE | LOSS
CONE

LOG $f(\alpha)$

0°   90°

LOCAL PITCH ANGLE α
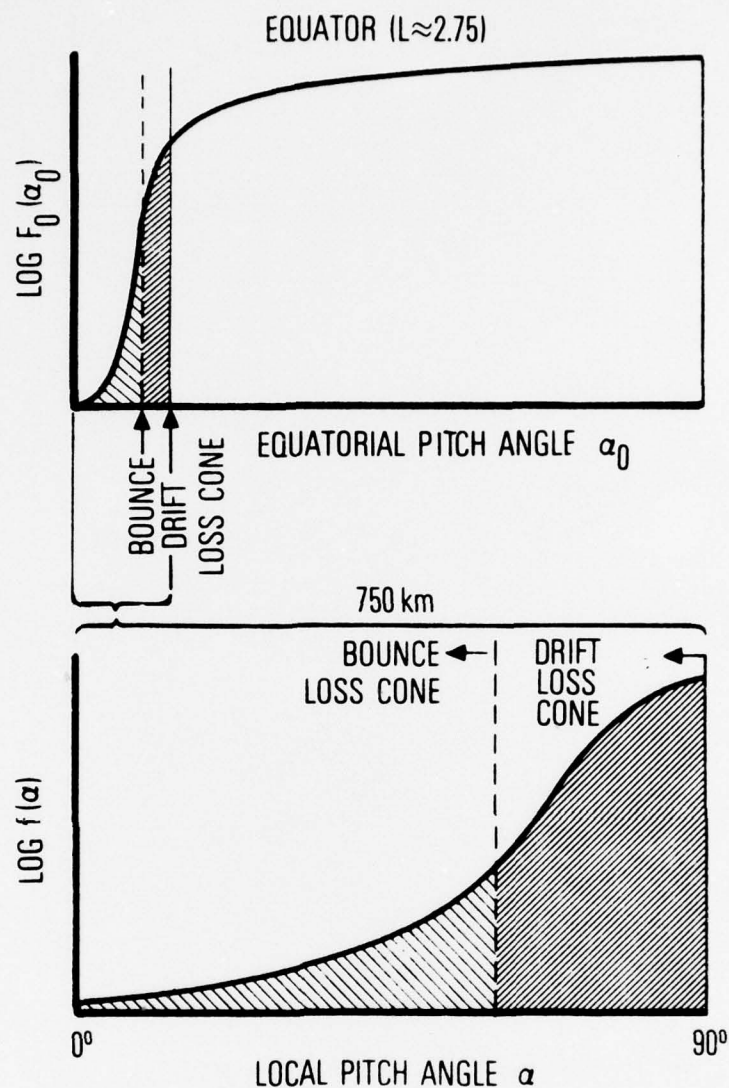
Figure 2.   Equatorial Pitch Angle Distribution at
L ≈ 2.75 (top) and Corresponding Distri-
bution at 750 km (bottom). The brackets
show that the particles that reach at
least 750 km before they mirror lie in a
small equatorial pitch angle range. All
of the particles observed at 750 km are
therefore in the drift loss cone. The
bounce loss cone is contained within the
drift loss cone.

-13-

II. MODEL FOR MIDLATITUDE PRECIPITATION

Assume that strong diffusion (Kennel and Petschek, 1966) occurs in a localized region of the magnetosphere near 0800 LT. Furthermore, assume that this region extends radially from an L value of at least 2 out of the plasmapause. Figure 3 illustrates this geometry schematically. The cross hatched area represents the source region.

Consider electrons that are scattered into the drift loss cone in the source region. An electron with a pitch angle within the local bounce loss cone precipitates immediately beneath the source. In the absence of further diffusion above the atmosphere, a quasitrapped electron drifts eastward until it encounters a location where its pitch angle is inside of the atmospheric sink. If the source is localized as shown in Figure 3, some predictions can be made about the temporal and spatial dependence of this combined precipitation.
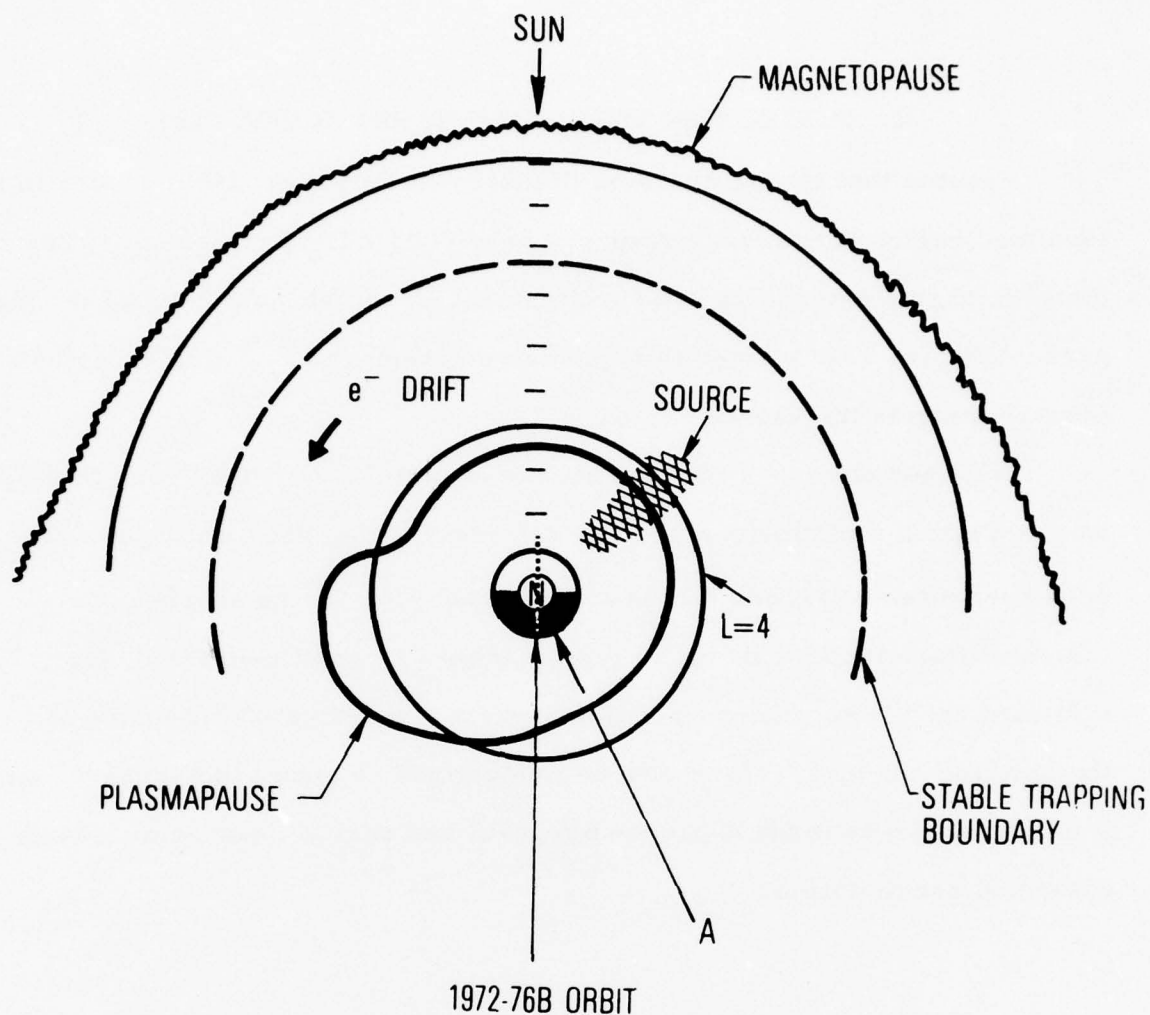
-15-

Figure 3. Schematic Showing a Polar View of the Magnetosphere.
The hypothetical morning source region is indicated by
the crosshatching. A typical orientation of the satellite
1972-76B and the anomaly A during data acquisition is
also indicated.

Figure 4a shows a hypothetical atmospheric loss cone curve for $L \approx 2$, modeled after Figure 1. An observer located at a fixed longitude point O corotates with the earth. The anomaly is located in the vicinity of longitude A. The morning source region, indicated by the crosshatched bar, moves across this curve once per day. Three source positions, corresponding to three different universal times, are illustrated. At the source, electrons are scattered into all pitch angles. Those with pitch angles within the loss cone angle at the source location will be precipitated directly at the source meridian. Electrons having a loss cone distribution (Kennel and Petschek, 1966) determined by the loss cone at the source will drift eastward from the source longitude. If the loss cone increases in the direction of electron drift, precipitation can occur east of the source up to the longitude where the loss cone stops growing. If the loss cone decreases in the direction of drift, the pitch angle distribution observed at O can reflect the loss cone size at the source longitude.

Figure 4b, case 1, illustrates the pitch angle distributions that would be observed at low altitude at O if the morning source were at the longitude T1 in Figure 4a. The center of symmetry is at 90° local pitch angle. The vertical dotted lines mark the maximum loss cone angle at the location of the observer. The part of the distribution between the dotted lines is trapped
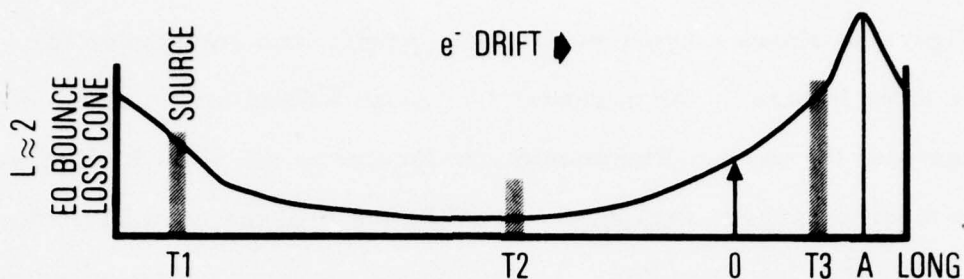
-17-

Figure 4a. Loss Cone Curve for $L \approx 2$ Showing the Location of the Anomaly Near A. An observer is at longitude O. The three crosshatched bars identify the location of the source region at three times.
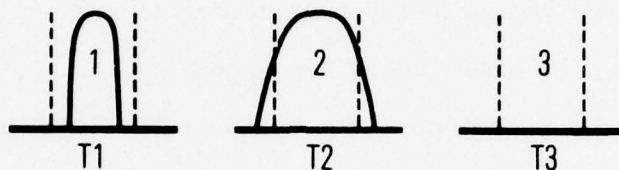
Figure 4b. Anticipated Low Altitude Pitch Angle Distributions for the Three Source Locations of 4a. Precipitation is occurring only at T2 where particles are present inside the local bounce loss cone.
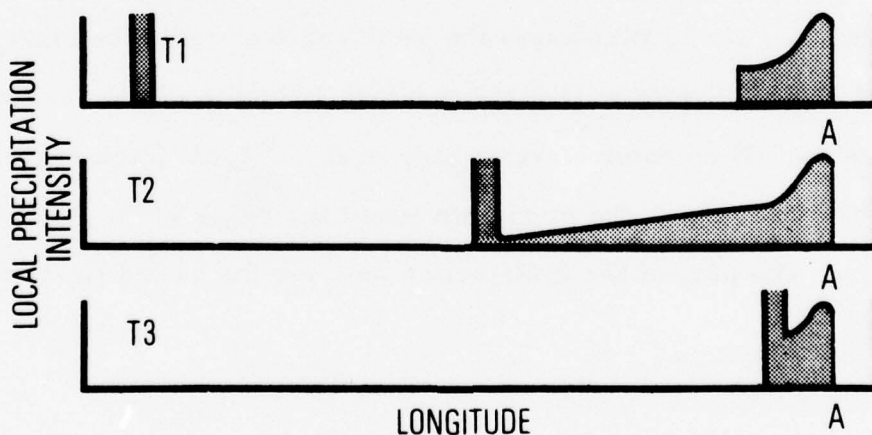

Figure 4c. Precipitation as a Function of Longitude for the Three Source Locations Shown. The amplitude of the shaded area, which is proportional to the eastward positive derivative of the loss cone curve 4a, should correlate with the intensity of precipitation.

at the longitude O. The part outside of these lines is precipitated into the atmosphere at the longitude O. In case 1, the atmospheric loss cone at the source is larger than the loss at the observer. A pitch angle distribution that is narrower than the local trapping limit is observed, and no precipitation into the atmosphere occurs at O.

In case 2, the loss cone at the source longitude T2 is smaller than the loss cone at O. In addition, the loss cone between the source and O is never greater than the loss cone angle at O. Thus, electrons with pitch angles inside of the local atmospheric loss cones are present at O. These are dumped into the atmosphere at the longitude of O in the hemisphere in which the loss cone is increasing most rapidly.

The alternative represented in case 3 of Figure 4b occurs whenever the anomaly is located between the source and the observer in the path of the electron drift. All of the drift loss cone particles are then precipitated into the atmosphere before they reach O.

In general, the longitude dependence of precipitation at points removed from the source location is determined by the rate at which the loss cone size increases in the direction of drift between the source and the anomaly. Figure 4c shows this derivative as a function of longitude for the three source locations discussed above. These curves, which are analogous to Figure 3 of Torr et al. (1975), give a qualitative picture of the $L \approx 2$ electron precipitation pattern at the three different times defined by the source locations in Figure 4a.

Data such as those shown in Figure 4c can be generated for all times and L values. In order to give a comprehensive view of midlatitude precipitation from a localized source, a model was adopted in which 1)the

-19-

source was represented by a delta function at 0800 LT, and 2) a realistic model of the magnetosphere (IAGA, 1969, Hilton, H. private communication) was used to provide the rate of the atmospheric loss cone increase in the direction of electron drift. The positive derivatives of the loss cone size, which correlate with the precipitation rate, were computed for several L values between 2 and 4. Separate curves were generated for the Northern and Southern Hemispheres, based on the assumption that precipitation occurs in the hemisphere in which the loss cone angle is increasing most rapidly. These numerical data were used to construct contour diagrams of universal time vs. longitude vs. precipitation rate.

A typical result is shown in Figure 5. The degree of shading is correlated with the amplitude scale of Figure 4c. The darkest areas show the times and locations of maximum precipitation of drift loss cone electrons into the atmosphere. As expected, the most intense precipitation occurs directly below the source in both hemispheres and also near the longitude of the South Atlantic Anomaly. The southern hemisphere precipitation maximum becomes less pronounced as L increases, but it persists up to L ≈ 4. Another small precipitation region appears in the Northern Hemisphere just east of the source region. Here the northern loss cone is increasing toward the east, causing some weak electron precipitation over China near zero hours UT. Most importantly, Figure 5 demonstrates that localizing the source of quasitrapped electrons introduces a time dependence into their precipitation pattern. Of course, these diurnal variations beome less pronounced for a source region that is not so extremely localized.
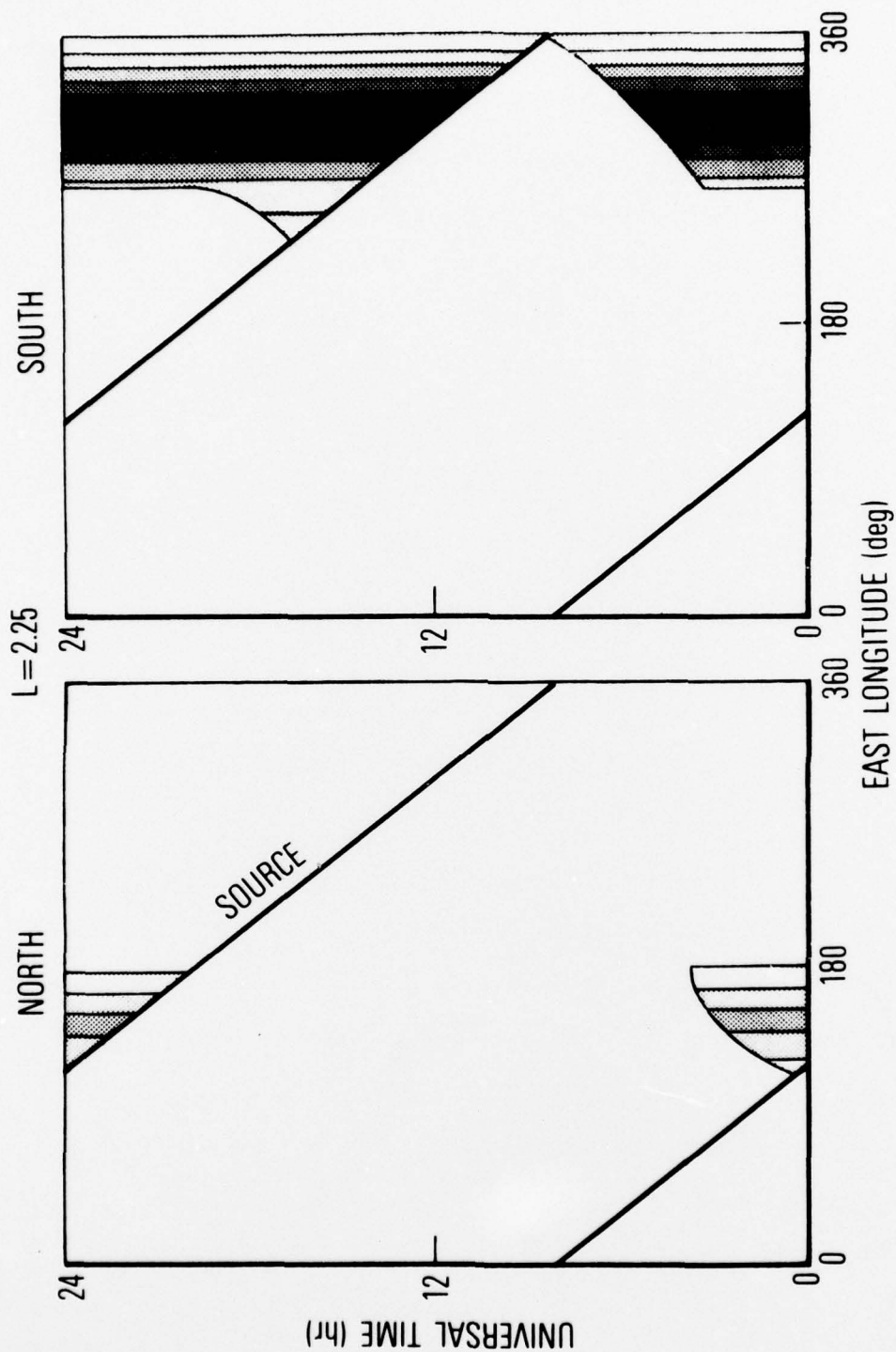
-20-

Figure 5. Contour Diagram Showing the Precipitation Intensity at Various Longitudes and Times at L ≈ 2.25 If a Delta Function Source of Quasitrapped Electrons Is Located at 0800 LT. Shading correlates with the amplitude scale of Figure 4c. Some precipitation always occurs directly below the source.

III. DISCUSSION

It is difficult to compare the present model with exiting mid-latitude data because experimenters do not usually treat time as a coordinate. However, some electron pitch angle distributions were available from a magnetic spectrometer on the low altitude satellite 1972-76B (Vampola, 1969). These data, although limited by the satellite orbital parameters and data acquisition plan, provided a test for the predictions of Figure 4b.

Figure 6 shows the regions in longitude-time space at $L \approx 2.25$ where the three types of pitch angle distributions of Figure 4b should be observed. The half-tone, black and white areas correspond to cases 1, 2 and 3 of Figure 4b respectively. The crosshatching shows where and when the pitch angle distributions are expected to exhibit the loss cone at the source rather than the local loss cone. The stipling shows where the distributions will be type 1 but will not be determined by the loss cone at the source. Here the source distributions have been modified by an increasing then decreasing loss cone during their drift history.

Pitch angle distributions from 1972-76B were available for a restricted area of Figure 6. The polar orbit and telemetry considerations generally provided observations for the satellite-anomaly-source-configuration illustrated in Figure 3. The data analysis covered several inactive periods during 1972-1974 when the D_{st} index indicated a quiet inner magnetosphere.

A typical pitch angle distribution obtained near 750 km in the crosshatched region is shown in Figure 7. A cosmic ray background level of about .5 counts/sec has been subtracted. The distribution appears narrower than the local atmospheric loss cone limit as predicted by Figure 4b case 1. The few counts in the local loss cone are probably a background effect. To verify that this shape was not a result of the data reduction scheme, pitch

Figure 6.   Longitude-Time Regions Where the Three Different
            Pitch Angle Distributions of Figure 4b Are Observed
            at L ≈ 2.25.   Type 1 distributions are seen in the
            crosshatched areas.   The large crosshatching indi-
            cates where the pitch angle distribution should
            exhibit the loss cone at the source location.   In the
            stippled area, the source distribution has been
            modified by the windshield wiper effect.   Type 2
            distributions, and precipitation, are found in the
            black regions.   The white areas contain empty
            (type 3) distributions.   Half-tone points indicate
            observations of narrow distributions, and open points
            show where empty distributions are observed in
            29 keV and 59 keV data.   The black points indicate
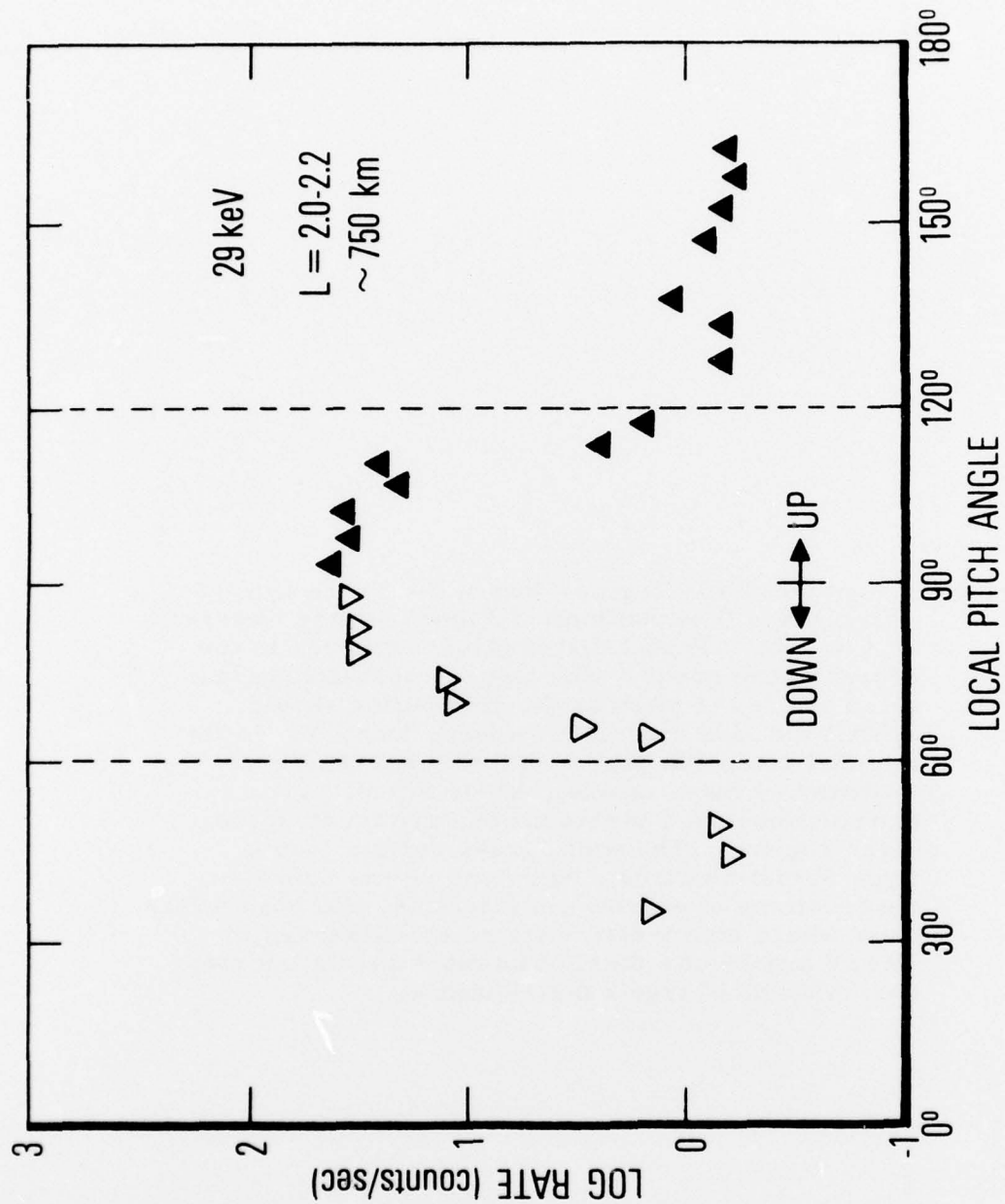   observations of type 2 distributions.

Figure 7. Example of a Narrow Pitch Angle Distribution (Type 1) Observed in the Large Crosshatched Area of Figure 6. Vertical dashed lines mark the local loss cone. These data have not been corrected for the ~17° width angular response of the detector.

angle distributions in the entire L range between 2 and 5 were examined. Some sequences of distributions for 29 keV and 59 keV electrons are shown in Figure 8. In keeping with the predictions of the present model, the narrow shape emerges only at the lower L values where the anomaly and localized morning source are effective. Moreover, for the data shown, the equatorial loss cone at 0800 LT was approximately 3 degrees greater than the local equatorial loss cone. This difference in equatorial loss cone corresponds to approximately 20 degrees at 750 km. A loss cone that is about 20 degrees larger than the local loss cone appears consistent with the shape of the narrow distributions.

A distribution representative of the black area is shown in Figure 9. In this case, corresponding to Figure 4b-2, the distribution appears to be determined by the local loss cone. Apparently, some of the electrons observed in the local loss cone are precipitating below the satellite. However, because the distributions in Figures 7-9 have been smoothed somewhat by the angular response of the detector, a quantitative measure of the precipitation cannot be made with confidence.

The data that were obtained in the white zone of Figure 6 generally appear isotropic at the low level of the cosmic ray background. There is only occasional evidence of a contribution from locally trapped electrons, as anticipated in Figure 4c.

The results of the data analysis are summarized in Figure 6. Half-tone points show where narrow (type 1) distributions were observed at L=2.25. Black and open points indicate observations of full (type 2) and empty (type 3) distributions respectively. This data sample, though limited, generally appears to be consistent with the scheme proposed above. Some disparity is expected
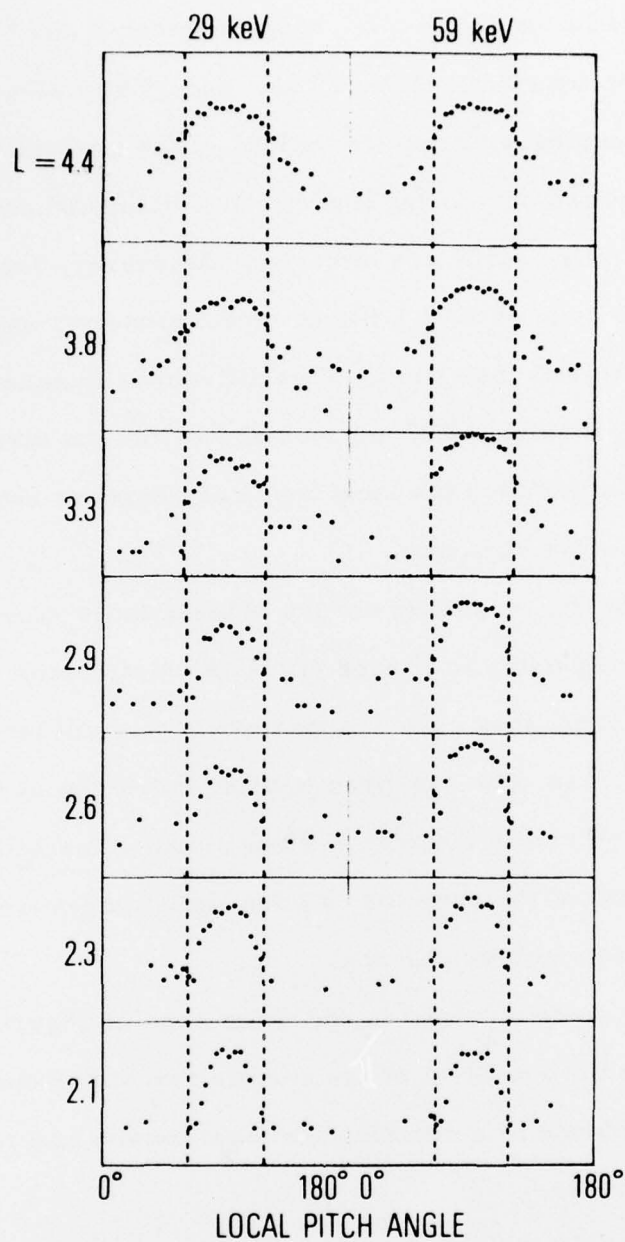
-27-

Figure 8.   Sequentially Observed Pitch Angle
Distributions Showing How the Shape
Evolves With L.   Narrow (type 1)
distributions emerge at $L \approx 3.5$ where
the localized source and anomaly sink
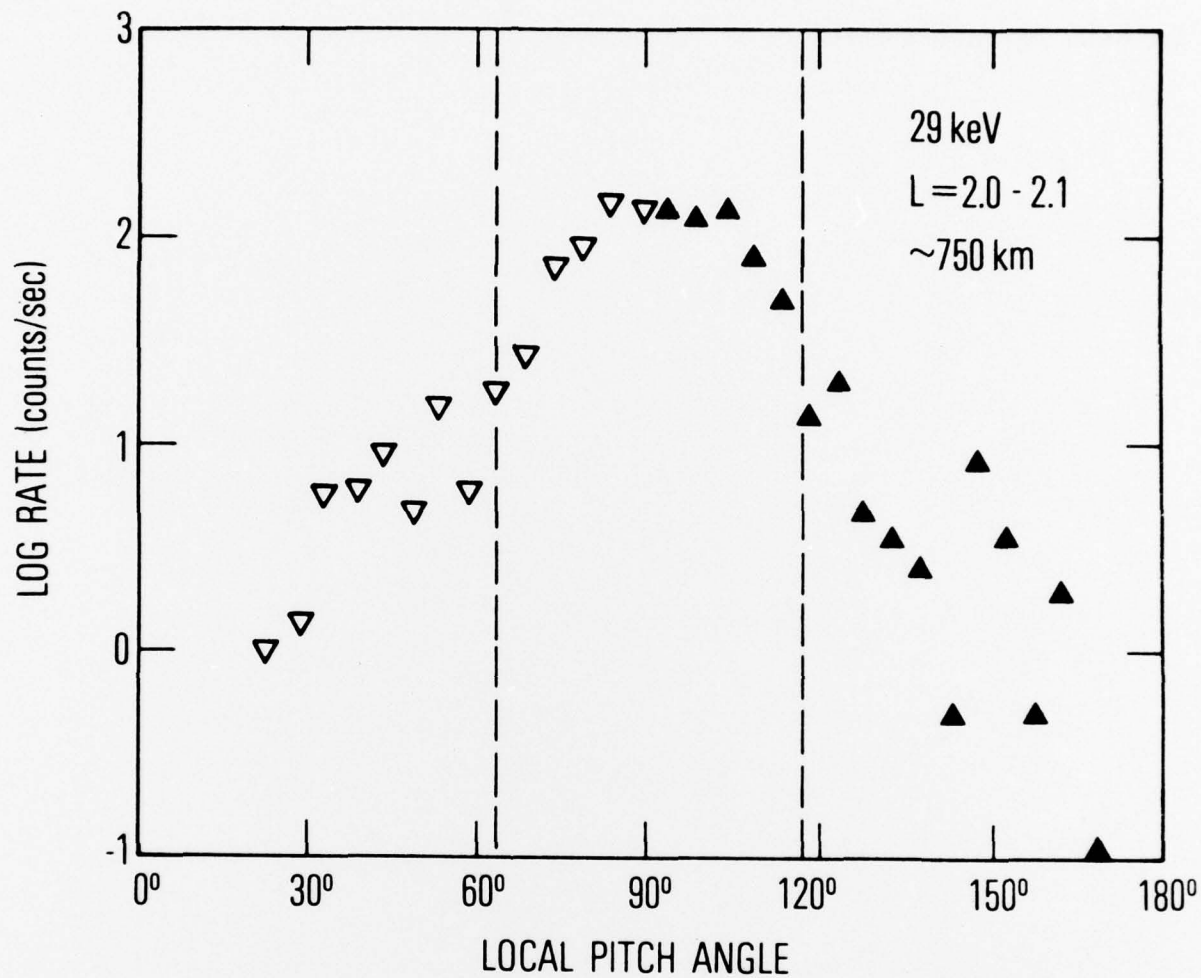model applies.

-28-

Figure 9. Example of a Type 2 Distribution Observed in the Black Area of Figure 6. These data have not been corrected for the angular response of the detector.

at the boundaries of the map because the local time and spatial extent
of the actual source region is only roughly approximated by the 0800
LT delta function model.

IV. CONCLUSIONS

Some previous experiments, including observations of electrons and of ELF chorus, suggest that a localized morning source supplies drift loss cone electrons at midlatitudes. Motivated by these results, a model was constructed in order to examine the consequences of a localized morning source. Quiet-time low altitude electron data were shown to be consistent with this model, which invoked a source of narrow longitudinal extent at 0800 LT. Further verification that quasitrapped electrons are generated in a narrow source region will require comprehensive samples of low altitude pitch angle distributions, observations of localized electromagnetic turbulence at L values between 2 and 4, and evidence that the well known windshield wiper effect has a diurnal variation.

In addition to providing a picture of midlatitude precipitation, the analysis described here provides further evidence that wave-particle interactions with the observed electromagnetic modes can dominate the behavior of kilovolt plasmasphere electrons. In particular, the quiet-time morning source model pieces together the independent observations of dawn-side plasma convection, morning electromagnetic noise maxima and quasitrapped electron behavior heretofore reported by various authors. Moreover, through the introduction of time dependence it provides a possible explanation for the sometimes erratic observations of precipitation-related phenomena in the South Atlantic Anomaly.

REFERENCES

Brice, N. and C. Lucas, Influence of magnetospheric convection and polar wind loss of electrons from the outer radiation belt, J. Geophys. Res., 76, 900, 1971.

Dunckel, N., and R. A. Helliwell, Whistler-mode emissions on the OGO 1 satellite, J. Geophys. Res., 74, 6371, 1969.

IAGA Commission 2, Working Group 4 (Analysis of the Geomagnetic Field), International geomagnetic reference field 1965.0, J. Geophys. Res., 74, 4407, 1969.

Imhof, W. L., Electron precipitation in the radiation belts, J. Geophys. Res., 73, 4167, 1968.

Imhof, W. L., E. E. Gaines and J. B. Reagan, Local time dependence of the loss of energetic electrons from the slot region of the radiation belts, J. Geophys. Res., 81, 291, 1976.

Kennel, C. F. and H. E. Petschek Limit on stably trapped particle fluxes, J. Geophys. Res., 71, 1, 1966.

Lyons, L. R., R. M. Thorne and C. F. Kennel, Pitch-angle diffusion of radiation belt electrons within the plasmasphere, J. Geophys. Res., 77, 3455, 1972.

Lyons, L. R. and D. J. Williams, the quiet time structure of energetic (35-560 keV) radiation belt electrons, J. Geophys. Res., 80, 943, 1975.

Mannan, J. D., B. T. Tsurutani and E. J. Smith, Distribution of ELF chorus with local time, latitude and magnetic activity, E S Trans, Am. Geophys. Union, 56, 424, 1975.

Paulikas, G. A., Precipitation of particles at low and middle latitudes, Rev. Geophys. Space Phys., 13, 709, 1975.

Roederer, J. G., Dynamics of Geomagnetically Trapped Radiation, Springer-Verlag, New York, 1970.

Taylor, W. L. and D. A. Gurnett, Morphology of VLF emissions observed with the Injun 3 satellite, J. Geophys. Res., 73, 5615, 1968.

Torr, D. G., M. R. Torr, J. C. G. Walker and R. A. Hoffman, Particle precipitation in the South Atlantic Geomagnetic Anomaly, Planet. Space Sci., 23, 15, 1975.

Tsurutani, B. T., E. J. Smith and R. M. Thorne, Electromagnetic hiss and relativistic electron losses in the inner zone, J. Geophys. Res., 74, 1254, 1969.

Vampola, A. L., H. C. Koons and D. A. McPherson, Outer-zone electron precipitation, J. Geophys. Res., 76, 7609, 1971.

Williams, D. J. and J. W. Kohl, Loss and replenishment of electrons at middle latitudes and high B values, J. Geophys. Res., 70, 4139, 1965.

THE IVAN A. GETTING LABORATORIES

The Laboratory Operations of The Aerospace Corporation is conducting experimental and theoretical investigations necessary for the evaluation and application of scientific advances to new military concepts and systems. Versatility and flexibility have been developed to a high degree by the laboratory personnel in dealing with the many problems encountered in the nation's rapidly developing space and missile systems. Expertise in the latest scientific developments is vital to the accomplishment of tasks related to these problems. The laboratories that contribute to this research are:

Aerophysics Laboratory: Launch and reentry aerodynamics, heat transfer, reentry physics, chemical kinetics, structural mechanics, flight dynamics, atmospheric pollution, and high-power gas lasers.

Chemistry and Physics Laboratory: Atmospheric reactions and atmospheric optics, chemical reactions in polluted atmospheres, chemical reactions of excited species in rocket plumes, chemical thermodynamics, plasma and laser-induced reactions, laser chemistry, propulsion chemistry, space vacuum and radiation effects on materials, lubrication and surface phenomena, photosensitive materials and sensors, high precision laser ranging, and the application of physics and chemistry to problems of law enforcement and biomedicine.

Electronics Research Laboratory: Electromagnetic theory, devices, and propagation phenomena, including plasma electromagnetics; quantum electronics, lasers, and electro-optics; communication sciences, applied electronics, semiconducting, superconducting, and crystal device physics, optical and acoustical imaging; atmospheric pollution; millimeter wave and far-infrared technology.

Materials Sciences Laboratory: Development of new materials; metal matrix composites and new forms of carbon; test and evaluation of graphite and ceramics in reentry; spacecraft materials and electronic components in nuclear weapons environment; application of fracture mechanics to stress corrosion and fatigue-induced fractures in structural metals.

Space Sciences Laboratory: Atmospheric and ionospheric physics, radiation from the atmosphere, density and composition of the atmosphere, aurorae and airglow; magnetospheric physics, cosmic rays, generation and propagation of plasma waves in the magnetosphere; solar physics, studies of solar magnetic fields; space astronomy, x-ray astronomy; the effects of nuclear explosions, magnetic storms, and solar activity on the earth's atmosphere, ionosphere, and magnetosphere; the effects of optical, electromagnetic, and particulate radiations in space on space systems.

THE AEROSPACE CORPORATION
El Segundo, California

• • •